How to cite: *Angew. Chem. Int. Ed.* **2024**, *63*, e202406848
doi.org/10.1002/anie.202406848

Polymer Chemistry

Aluminum Alkyl Induced Isomerization of Group IV *meso* Metallocene Complexes

*Tim M. Lenz, Ion Chiorescu, Fabrizio E. Napoli, Jin Y. Liu, and Bernhard Rieger**

Abstract: The synthesis of group IV metallocene precatalysts for the polymerization of propylene generally yields two different isomers: The *racemic* isomer that produces isotactic polypropylene (iPP) and the *meso* isomer that produces atactic polypropylene (aPP). Due to its poor physical properties, aPP has very limited applications. To avoid obtaining blends of both polymers and thus diminish the mechanical and thermal properties of iPP, the *meso* metallocene complexes need to be separated from the *racemic* ones tediously—rendering the metallocene-based polymerization of propylene industrially far less attractive than the *Ziegler*/*Natta* process. To overcome this issue, we established an isomerization protocol to convert *meso* metallocene complexes into their *racemic* counterparts. This protocol increased the yield of iPP by 400 % while maintaining the polymer's excellent physical properties and was applicable to both hafnocene and zirconocene complexes, as well as different precatalyst activation methods. Through targeted variation of the ligand frameworks, methoxy groups at the indenyl moieties were found to be the structural motifs responsible for an isomerization to take place—this experimental evidence was confirmed by density functional theory calculations. Liquid injection field desorption ionization mass spectrometry, as well as ^{1}H and ^{29}Si nuclear magnetic resonance studies, allowed the proposal of an isomerization mechanism.

Introduction

The discovery of the coordinative polymerization of ethylene and propylene by *Ziegler* and *Natta* in the 1950s marked arguably the most crucial breakthrough in polymer research to this date.[1] 30 years later, *Brintzinger* and *Kaminsky* established well-defined single-site, homogeneous *ansa*-zirconocene complexes for the iso-selective polymerization of propylene.[2] Using methylaluminoxane (MAO) as a co-catalyst, they were able to produce polypropylene with far higher molecular weights and more narrow molecular weight distributions than the *Ziegler*/*Natta* systems based on $TiCl_4$/ID/$MgCl_2$ (ID = internal electron donor). Nowadays, research regarding the homogeneous polymerization of propylene still relies on this pioneering work. However, maximizing the catalyst performance, as well as the stereoregularity and molecular weight of the produced polymer, became the main focus, and novel techniques such as high-throughput experimentation are being established to achieve these goals.[3] When it comes to highly isotactic polypropylene, indenyl-based metallocenes play a crucial role. Using the ultra-rigid *ansa*-hafnocene complex *rac*-$\mathbf{I_{Hf}}$, our group was able to produce iPP with the highest melting transition temperature *ex reactor* to this date.[4] One issue regarding not only our benchmark catalyst but all indenyl-based metallocene precatalysts is the laborious and sometimes impossible separation of the *racemic* (*rac*) and *meso* isomers of these complexes.[5] While the *racemic* metallocene species yield isotactic polypropylene (iPP), their *meso* analogs are known to produce undesired atactic polypropylene (aPP) according to *Ewen's* symmetry rules.[6] Since generally, both isomers are formed upon attachment of the ligand to the central metal atom, obtaining the *racemic* isomers in a very pure manner is mandatory before any precatalyst can be considered suitable for the iso-selective polymerization of

[*] T. M. Lenz, J. Y. Liu, Prof. Dr. B. Rieger
Wacker-Lehrstuhl für Makromolekulare Chemie
Catalysis Research Center
Technische Universität München
TUM School of Natural Sciences
Lichtenbergstraße 4, 85748 Garching
Garching bei München (Germany)
E-mail: rieger@tum.de

Dr. I. Chiorescu
Department Chemie
Technische Universität München
TUM School of Natural Sciences
Lichtenbergstraße 4, 85748 Garching
Garching bei München (Germany)

F. E. Napoli
Lehrstuhl für Anorganische und Metallorganische Chemie
Catalysis Research Center
Technische Universität München
TUM School of Natural Sciences
Lichtenbergstraße 4, 85748 Garching
Garching bei München (Germany)

propylene. This purification usually consists of several fractional crystallizations of the complexes and thus diminishes the yield of the *racemic* isomer; furthermore, considerable amounts of the precious ligands are wasted in the form of discarded *meso* isomers. Considering the expensive and time-consuming preparations of metallocene precatalysts, this fact contributes to the industrial unprofitability of the homogeneous polymerization of propylene. Even though some protocols exist to convert *meso* metallocene complexes into their *racemic* analogs, their applicability is limited as they often reach an equilibrium state between both isomers, and they add an additional, labor-consuming purification step to the precatalyst syntheses.[7] Recently, we reported the isomerization of hafnocene complex *meso*-$\mathbf{I_{Hf}}$ upon conversion with 1.00 equivalent (eq.) of triisobutylaluminum (TIBA).[8] The subsequent in situ activation using 200 eq. TIBA and 5.00 eq. $[Ph_3C][B(C_6F_5)_4]$ (TrBCF) afforded perfectly isotactic polypropylene with macromolecular characteristics analog to polypropylene produced by the pure *racemic* isomer.

In this work, we optimized the isomerization conditions regarding TIBA concentration, reaction temperature, and time, thus achieving a more thorough isomerization. We explored the structural motif responsible for the isomerization and postulated a reaction mechanism based on density functional theory (DFT) calculations, as well as liquid injection field desorption ionization mass spectrometry (LIFDI-MS) and various nuclear magnetic resonance (NMR) experiments. Currently, both research and industry prefer zirconocene complexes for the production of polypropylene, while their heavier analogs experience far less attention.[9] For this reason, we extended the scope of the isomerization protocol to different zirconocene/MAO systems but also structurally assorted hafnocene complexes proven by ^{1}H and ^{29}Si NMR studies.

Results and Discussion

Complex Syntheses

The isomerization behavior of complex *meso*-$\mathbf{I_{Hf}}$ upon TIBA addition was investigated thoroughly in our previous work.[8] To identify the structural motifs of the ligand framework responsible for the isomerization to occur, the hafnocene complexes *meso*-$\mathbf{I_{Hf}}$–$\mathbf{V_{Hf}}$, as well as their corresponding zirconocene analogs *meso*-$\mathbf{I_{Zr}}$–$\mathbf{V_{Zr}}$ were synthesized, and their reactions upon TIBA addition were evaluated (Scheme 1).

The syntheses of complexes **I–V** afforded isomeric mixtures ranging from *rac*/*meso* 2/1 to pure *meso*, depending on each individual precatalyst. The presence of *racemic* isomers did not affect the isomerization behavior of the corresponding *meso* species. Therefore, we did not isolate the pure *meso* isomers of all complexes. Complexes $\mathbf{II_{Zr}}$, $\mathbf{III_{Hf}}$, and $\mathbf{IV_{Hf}}$ have previously not been reported in the literature. Their synthesis was carried out analog to the literature-known analogs and afforded *rac*/*meso* mixtures.[3b,10] The *racemic* isomers were separated through fractional crystallization and thoroughly characterized using ^{1}H, ^{13}C, and ^{29}Si NMR spectroscopy, as well as LIFDI-MS. $\mathbf{II_{Zr}}$ was additionally characterized using single-crystal X-ray diffraction (SC-XRD).[11] Complex $\mathbf{V_{Hf}}$ has previously been reported in the literature,[12] however, was never thoroughly characterized to the best of our knowledge. Thus, we carried out its characterization using NMR, MS, and SC-XRD.

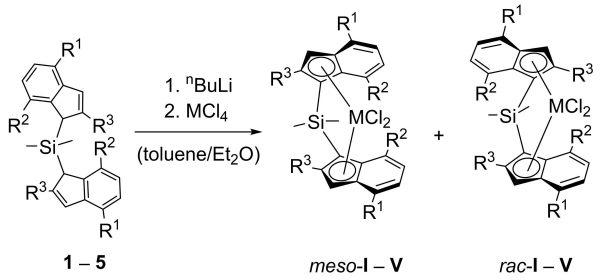

1 / I: R^1 = (3,5-di-tert-butyl)-phenyl; R^2 = OMe; R^3 = Me
2 / II: R^1 = Ph; R^2 = OMe; R^3 = Me
3 / III: R^1 = Ph; R^2 = H; R^3 = Me
4 / IV: R^1 = H; R^2 = H; R^3 = Me
5 / V: R^1 = H; R^2 = H; R^3 = H
M: Zr, Hf

Scheme 1. Syntheses of metallocene complexes **I–V**.

Optimization of Isomerization Conditions

In our previous work, isomerization experiments were carried out dissolving the metallocene complex and 1.00 eq. TIBA in toluene with the mixtures being heated to 100 °C for 16 hours for complete conversion from *meso* to *rac*. This procedure, however, afforded small amounts of side products visible in the ^{1}H NMR spectra of the isomerized complexes.[8] While these side products did not affect the polymerization performance of the activated catalysts, we still aimed to achieve an entirely clean isomerization to maximize the yield of the *racemic* isomers and, thus, the later-produced isotactic polypropylene. We therefore optimized the isomerization conditions and found that side products could be avoided by reducing the amount of TIBA to 0.50 eq. and increasing the reaction temperature to 120 °C; conversions were monitored using ^{1}H NMR spectroscopy. Sixteen hours of reaction time were necessary for a complete conversion of complex *meso*-$\mathbf{I_{Hf}}$, while only one to four hours were required for complexes *meso*-$\mathbf{I_{Zr}}$, *meso*-$\mathbf{II_{Hf}}$, and *meso*-$\mathbf{II_{Zr}}$. The absence of other signals besides the *racemic* products in the ^{29}Si NMR spectra proved an actual isomerization of the complexes to the corresponding *racemic* species took place—not just a degradation of the *meso* isomers (Scheme 2). Direct comparison of the respective metallocene complexes revealed that the isomerization of zirconocene complexes tended to occur faster (3 h for *meso*-$\mathbf{I_{Zr}}$ and 1 h for *meso*-$\mathbf{II_{Zr}}$) than the isomerization of the corresponding hafnocene analogs (16 h for *meso*-$\mathbf{I_{Zr}}$ and 4 h for *meso*-$\mathbf{II_{Zr}}$). Trimethylaluminum (TMA) was also suitable

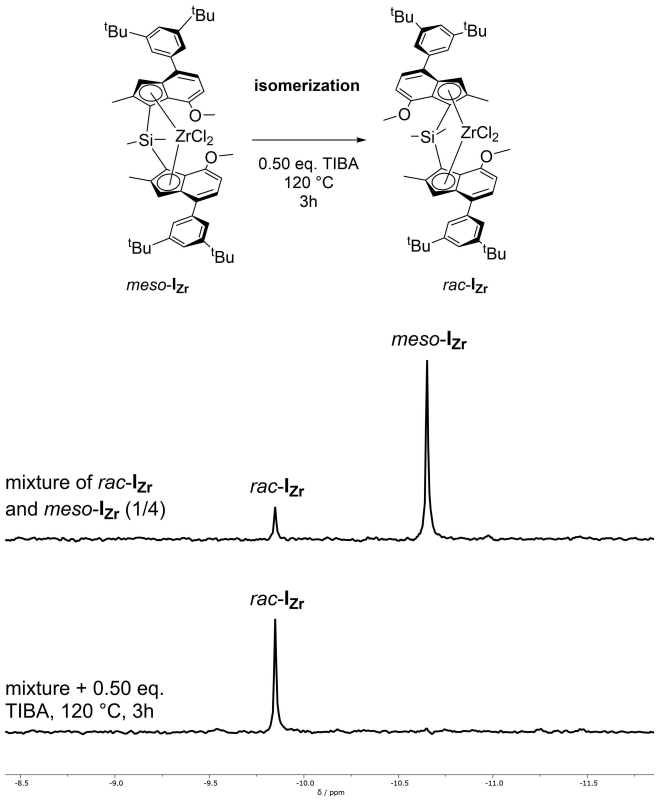

Scheme 2. Excerpts of the ^{29}Si NMR spectra of a mixture of *rac*-$\mathbf{I}_{Zr}$ and *meso*-$\mathbf{I}_{Zr}$ before and after isomerization according to the depicted reaction using 0.50 eq. TIBA at 120 °C for 3 h. Full spectra for all isomerization experiments are provided in the Supporting Information.

to isomerize these *meso* complexes; however, due to the known fact that TMA severely hampers the activity of hafnocene complexes regarding the polymerization of propylene, it was only used for mechanistic studies and not for polymerization experiments.[13]

In the absence of TIBA or TMA, no isomerization was observed for complex *meso*-$\mathbf{I}_{Hf}$, while partial isomerization was observed for *meso*-$\mathbf{II}_{Hf}$, *meso*-$\mathbf{I}_{Zr}$, and *meso*-$\mathbf{II}_{Zr}$. However, the formation of side products was predominant in all of these control experiments. No isomerization was observed for complexes *meso*-**III**, *meso*-**IV**, and *meso*-**V** (M: Zr, Hf) under various conditions, proving that both the methoxy groups of the metallocene complexes, as well as the presence of an aluminum alkyl were crucial for an isomerization to take place. The role of both will be discussed later on.

Polymerization Experiments Using Isomerized Metallocene Complexes

To compare the polymerization performances of isomerized *meso*-**I** and *meso*-**II** (M: Zr, Hf), as well as their *racemic* analogs, propylene polymerizations were carried out. The resulting polymers were characterized according to their molecular weight, stereoregularity, and melting transition temperature (Table 1).

Polymerizations involving hafnocene complexes were conducted using the in situ activation method with TIBA/TrBCF in analogy to our previous work. As evidenced by Table 1, the isomerization of *meso*-$\mathbf{I}_{Hf}$ and *meso*-$\mathbf{II}_{Hf}$ and subsequent in situ activation yielded iPP with equal properties to iPP produced from the corresponding pure *racemic* isomers, proving a complete isomerization. Contrary to hafnocene complexes, which are usually insufficiently activated when MAO is used,[13] zirconocene precatalysts can easily be activated with MAO; this activation is generally more frequently employed.[9a,14] Thus, in addition to the in situ activation of hafnocene complexes, we aimed to extend our isomerization/polymerization protocol to zirconocene complexes, subsequently activated with MAO. iPP obtained from the isomerized zirconocene complexes *meso*-$\mathbf{I}_{Zr}$ and *meso*-$\mathbf{II}_{Zr}$, which were activated with MAO, exhibited the same macromolecular characteristics as iPP produced by the direct MAO activation of the corresponding *racemic* isomers. Evidently, the MAO activation worked just as well for previously isomerized zirconocene complexes and was additionally not hampered by residual TIBA used for the isomerization. Many commercially available MAO solutions are enhanced through the addition of TIBA, anyway.[15] In our previous work,[8] we showed that the direct addition of

Table 1: Conditions and results for the polymerization of propylene with complexes *rac*/*meso*-**I** and **II** (M: Zr, Hf).[a]

entry	precatalyst	n[b]	activation[c]	T_{Polym}[d]	t_{Polym}[e]	[mmmm] [f]	M_w[g]	$Đ$[h]	T_m[d]	P[i]
1[7]	*rac*-$\mathbf{I}_{Hf}$	1.65	TIBA/TrBCF	30	30	>99	1600	1.6	165	6000
2[7]	*rac*/*meso*-$\mathbf{I}_{Hf}$ (1/4) [j]	1.65	TIBA/TrBCF	30	30	>99	1300	1.6	165	5000
3	*rac*-$\mathbf{II}_{Hf}$	1.30	TIBA/TrBCF	30	15	99	500	1.8	160	1200
4	*rac*/*meso*-$\mathbf{II}_{Hf}$ (1/4) [j]	1.30	TIBA/TrBCF	30	15	>99	700	1.6	161	1000
5	*rac*-$\mathbf{I}_{Zr}$	1.64	MAO	30[k]	15	>99	700	2.9	159	32000
6	*rac*/*meso*-$\mathbf{I}_{Zr}$ (1/4) [j]	1.64	MAO	30	15	>99	800	2.5	159	30000
7	*rac*-$\mathbf{II}_{Zr}$	1.45	MAO	60	15	98	600	1.6	156	10000
8	*rac*/*meso*-$\mathbf{II}_{Zr}$ (1/4) [j]	1.45	MAO	60[k]	15	98	700	2.1	155	15000

[a] $V_{toluene}$ = 120 mL; $p = p_{Ar} + p_{propylene}$ = 4 bar, p_{Ar} = 1.5 bar. [b] In μmol. [c] TIBA/TrBCF: initiator $[Ph_3C][B(C_6F_5)_4]$ = 5.00 eq., activator (TIBA) = 200 eq., scavenger (TIBA) = 0.55 mmol; methylaluminoxane (MAO): scavenger = activator (MAO) = 2000 eq. [d] In °C. [e] In min. [f] In %, determined via ^{13}C NMR spectroscopy assuming the enantiomorphic site model. [g] In kg mol^{-1}, determined absolutely via SEC-GPC in 1,2,4-trichlorobenzene at 160 °C with dn/dc = 0.097 mL g^{-1}. [h] $Đ = M_w/M_n$. [i] in kg_{PP} $[mol_{cat}\,h]^{-1}$. [j] Pre-isomerized with 1.00 eq. (entry 2)/0.50 eq. (entry 4, 6, 8) TIBA at 120 °C. [k] ±10 °C.

MAO to *meso* metallocene complexes, however, led to the formation of atactic polypropylene which we attributed to MAO's ability to generate a free coordination site by itself. This highlights the necessity of a complete isomerization using either TIBA or TMA before MAO is employed.

One of the most considerable complications regarding polymerizations relying on metallocene precatalysts is that their syntheses yield *meso* and *racemic* isomers in ratios of up to 4/1.[8] The herein established isomerization/polymerization protocol circumvents the issue of wasting precious metallocene complexes for both hafnocene and zirconocene complexes, even for different activation methods, while maintaining the desired polymer properties.

Structural Motifs Responsible for the Isomerization

While the complexes *meso*-**I** and *meso*-**II** (M: Zr, Hf) were readily isomerized at 120 °C after the addition of 0.50 eq. TIBA, the complexes *meso*-**III**, *meso*-**IV**, and *meso*-**V** (M: Zr, Hf) exhibited no isomerization at temperatures ranging from 60 °C to 120 °C and TIBA concentrations ranging from 0.20 eq. to 10.0 eq. Moreover, no isomerization of the latter complexes employing the sterically less hindered TMA could be observed; in our previous work, we showed that this reagent was also suitable to induce an isomerization of meso-$\mathbf{I}_{Hf}$.[8] The isomerization phenomenon thus seems to be independent of the central metal atom—an observation that can be attributed to the inherent chemical similarity of hafnium and zirconium regarding their electronegativity, as well as atomic and ionic radii.[16] The results presented, however, suggest that the methoxy substituents at position 7 of the indenyl frameworks of the ligands are the crucial factors for an aluminum alkyl induced isomerization to take place. Independent of the steric demand of the aryl moieties, only *meso* metallocene complexes bearing these structural motifs underwent isomerization to their *racemic* analogs. Monitoring the isomerization using ^{1}H NMR spectroscopy, we did not observe changes in the chemical shifts of these methoxy groups—besides the differences between both isomers and the intermediates discussed below. We interpret these results as a hypothetical high-energy intermediate having a shorter lifetime than the NMR timescale and, thus, not being detectable via this analytical method.

Using DFT with the standard B3LYP functional (see Supporting Information for details), the energies required for ligands 2 and 3 to adapt the geometry they occupy in the respective *racemic* and *meso* hafnocene complexes were calculated (Figure 1).

40 kJ/mol are required to form each conformer of ligand **3** bearing no methoxy groups, rendering no conformation, *rac*-$\mathbf{III}_{Hf}$ or *meso*-$\mathbf{III}_{Hf}$, energetically favored. On the other hand, ligand 2 uses 40 kJ/mol to complexate Hf and yield *rac*-$\mathbf{II}_{Hf}$, but 59 kJ/mol to adapt the geometry as in *meso*-$\mathbf{II}_{Hf}$. The excess of energy is required to bend the aromatic groups at the silicon atom by ~10° from the 105° in the free ligand to the conformation with a central metal atom. Consequently, the *meso* isomer is destabilized by 19 kJ/mol relative to *rac*-$\mathbf{II}_{Hf}$, mostly as a result of the intramolecular

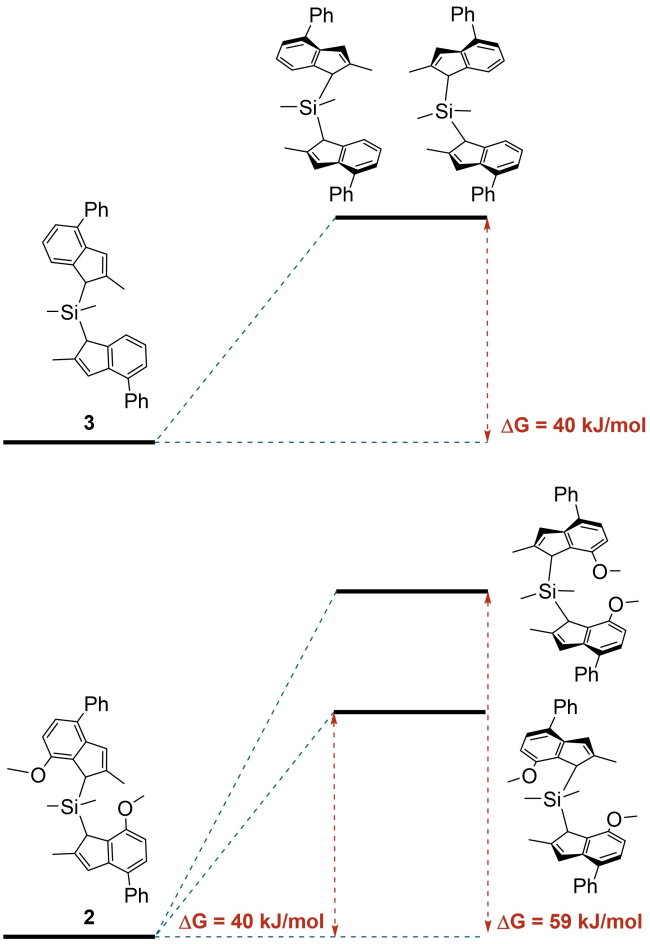

Figure 1. Energy diagrams of the transformation of ligands **2** and **3** into the conformers required to form the respective *racemic* and *meso* metallocene complexes.

stress in the complexated ligand 2 (Table S1). Therefore, the methoxy groups at position 7 of the indenyl framework are ultimately responsible for the isomerization, with the driving force being the relative thermodynamic stabilities of *meso* and *rac* conformations of metallocene complexes bearing these substituents. The reason for *meso*-**I** and *meso*-**II** (M: Zr, Hf) to be formed besides their *racemic* counterparts during the metallocene syntheses at all thus seems to be of kinetic origin. It is feasible that the di-lithiated species obtained by deprotonation of the bis(indenyl) precursors exhibit some lithium-oxygen chelation. Thus, a pre-orientation of both ligand sites before the transmetalation step involving the group IV metal halide seems to occur, yielding the thermodynamically less favored *meso* isomers by up to 80 %.

Isomerization Mechanism

While the energetic differences between the ligand conformations required for *meso*-$\mathbf{II}_{Hf}$ and *rac*-$\mathbf{II}_{Hf}$ to form explain the driving force of the isomerization, they yet fall short of elucidating the detailed reaction mechanism. Since

no thorough isomerization at 120 °C was observed in the absence of TIBA or TMA for any complex, an entirely thermal isomerization can be ruled out, and it becomes clear that the respective aluminum alkyl acts as a catalyst for the isomerization in some way.

To gain further insight into the isomerization mechanism, a kinetic ^{1}H NMR study and LIFDI-MS experiments of the conversion of *meso*-$\mathbf{I_{Hf}}$ with TMA were conducted. Since the latter method is not yet quite widespread, a brief overview of its functionality and its specific advantages in elucidating our isomerization mechanism is given in the Supporting Information. As visible via ^{1}H NMR, the isomerization proceeded via two different intermediates: A symmetric species formed from *meso*-$\mathbf{I_{Hf}}$ over the course of 90 min at 100 °C and an asymmetric one formed from this symmetric intermediate within four hours at 100 °C. To a certain extent, the latter species was then converted into *rac*-$\mathbf{I_{Hf}}$. This asymmetric species was stable under argon atmosphere (> 15 days), and removal of the overlaying solution, as well as residual TMA, under vacuum, did not lead to decomposition. In the ^{1}H NMR spectrum, the former, symmetric species exhibited a characteristic peak at δ = −1.28 ppm with a relative integral of 3, suggesting a Hf-methyl moiety. We therefore concluded this species to be the mono-methylated *meso*-$\mathbf{I_{Hf}Me}$ (Figure 2).

Besides the signal corresponding to *rac*-$\mathbf{I_{Hf}}$, the ^{29}Si NMR spectrum of the final reaction products (Figure S45) exhibited only one additional signal, proving that the mentioned asymmetric species was, in fact, one single species and not two symmetric ones with equal relative integrals. Moreover, the ^{1}H NMR spectrum of this species exhibited a signal at δ = −0.40 ppm with a relative integral of 3, suggesting another Hf-methyl moiety. We concluded this species to be *rac*-$\mathbf{I_{Hf}Me}$ (Figure 2); LIFDI-MS confirmed this assumption (Figure S50). Selected signals in the respective ^{1}H NMR spectra of *meso*-$\mathbf{I_{Hf}Me}$ and *rac*-$\mathbf{I_{Hf}Me}$ are depicted in Figure 2. The mentioned Hf-methyl groups, as well as the cyclopentadienyl (Cp)-methyl groups are highlighted, respectively.

The methyl groups at the Cp moieties of the metal complexes proved suitable for differentiating each species' relative amounts during the isomerization process. Excerpts of the corresponding ^{1}H NMR spectra of the kinetic NMR experiment in this spectral region are summarized in Figure 3.

The relative amounts of *meso*-$\mathbf{I_{Hf}Me}$, *meso*-$\mathbf{I_{Hf}}$, *rac*-$\mathbf{I_{Hf}}$, and *rac*-$\mathbf{I_{Hf}Me}$ were determined through integration of the signals highlighted in Figure 3. Plots of these amounts over the course of 90 minutes and 22 hours, respectively, are depicted in Figure 4.

We could also obtain *rac*-$\mathbf{I_{Hf}Me}$ through the direct reaction of *rac*-$\mathbf{I_{Hf}}$ with TMA; in this case, however, *meso*-$\mathbf{I_{Hf}Me}$ and *meso*-$\mathbf{I_{Hf}}$ were not detected as additional reaction products. Similarly, analog methylated, asymmetric products were also detectable in the respective ^{1}H NMR spectra when *rac*-$\mathbf{I_{Zr}}$, *rac*-$\mathbf{II_{Hf}}$, and *rac*-$\mathbf{II_{Zr}}$ were heated to 100 °C in the presence of TMA (Supporting Information). LIFDI-MS confirmed the molecular masses of the reaction products to match the calculated values for the corresponding methylated species.

In addition to the kinetic ^{1}H NMR experiment discussed above, we used LIFDI-MS to in situ monitor the reaction of *meso*-$\mathbf{I_{Hf}}$ with TMA. Excitingly, we observed a species with a mass equivalent to the combined masses of *meso*-$\mathbf{I_{Hf}}$ and TMA (Figure 5). Since field-desorption is a very soft ionization method, this species is most likely no artefact from the mass-spectrometric investigation, but an actual

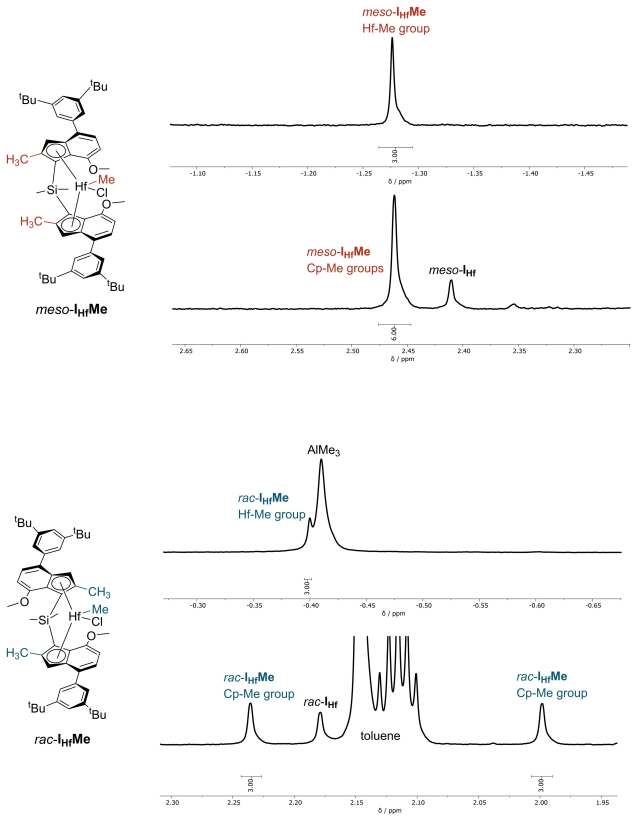

Figure 2. Excerpts of the ^{1}H NMR spectra of *meso*-$\mathbf{I_{Hf}Me}$ and *rac*-$\mathbf{I_{Hf}Me}$. The corresponding protons are highlighted in the depicted chemical structures. Full spectra are provided in the Supporting Information.

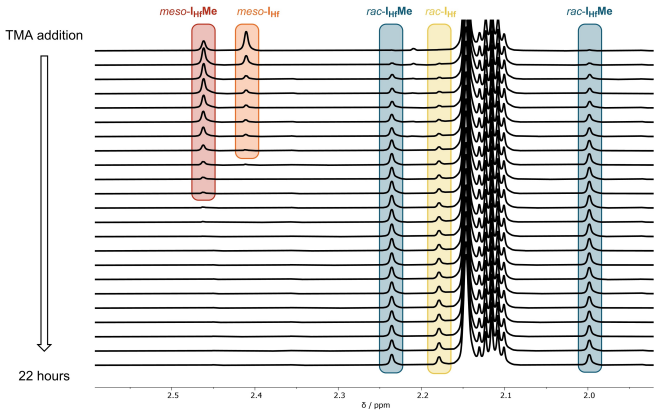

Figure 3. Excerpts of the ^{1}H NMR spectra of the conversion of *meso*-$\mathbf{I_{Hf}}$ with 2.00 eq. TMA at 100 °C. Full spectra are provided in the Supporting Information.

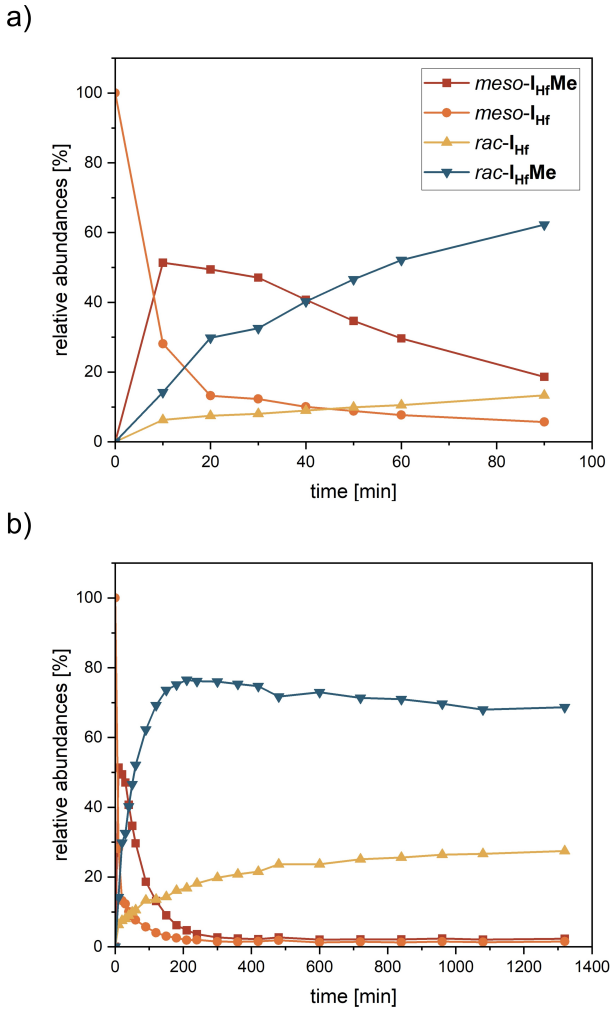

Figure 4. Relative abundances of meso-$\mathbf{I_{Hf}Me}$, meso-$\mathbf{I_{Hf}}$, rac-$\mathbf{I_{Hf}}$, and rac-$\mathbf{I_{Hf}Me}$ during the conversion of meso-$\mathbf{I_{Hf}}$ with 2.00 eq. TMA at 100 °C. For better visibility, plot a) is a zoomed depiction of the first 90 min of plot b). Abundances were determined by integration of the Cp-methyl groups.

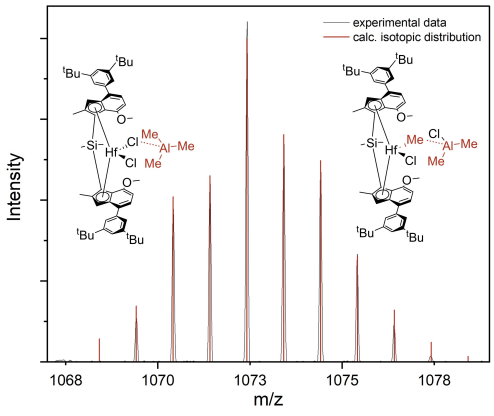

Figure 5. Calculated isotopic distribution and detected masses of *meso*-$\mathbf{I_{Hf}}$+TMA.

reaction product (see Supporting Information for a detailed explanation).

We thought three different structures for the complex/TMA interaction conceivable: The first and the one we consider most likely is depicted in Figure 5 and involves the interaction of TMA with the chloride substituents at the central metal atom—either before or after a methyl exchange reaction which will be discussed shortly. The other two possible coordination sites of the electrophilic TMA are the electron-rich Cp-rings, as well as the methoxy groups of *meso*-$\mathbf{I_{Hf}}$. According to DFT calculations on the complexes $\mathbf{II_{Hf}}$ and $\mathbf{III_{Hf}}$ (Table S2), all three interactions are feasible with none being energetically significantly preferred over another. However, the interaction with the chloride substituents is energetically at least slightly favored by up to 15 kJ/mol and 14 kJ/mol, respectively, compared to an interaction with the Cp-rings and the methoxy groups. Moreover, both other interactions do not significantly change the geometry around the central metal atom which would be a prerequisite for the respective species to be involved in the isomerization mechanism, whereas coordination of TMA to a chloride substituent elongates the respective Hf–Cl bond. Therefore, the following discussion will only focus on the TMA/chloride interaction.

The chloride/methyl exchange reaction of metallocene dichlorides with TMA via a $L_2ClHf(\mu\text{-}Cl)AlMe_3$ (L = ligand) species is reasonably well understood in the literature.[17] We performed DFT calculations of this reaction for *meso*/*rac*-$\mathbf{II_{Hf}}$ and the analog complex lacking the methoxy groups *meso*/*rac*-$\mathbf{III_{Hf}}$ (calculations were not conducted for $\mathbf{I_{Hf}}$ due to the fact that $\mathbf{II_{Hf}}$ contains significantly less atoms than $\mathbf{I_{Hf}}$ and both exhibited the same behavior, experimentally). The energetics of this reaction are summarized in Table S3 and indicate the parent species $L_2ClHf(\mu\text{-}Cl)AlMe_3$ to be energetically slightly favored over the corresponding methylated one $L_2ClHf(\mu\text{-}Me)AlMe_2Cl$ in each case. Methylation of *meso*-$\mathbf{II_{Hf}}$, however, is favored by 13 kJ/mol over methylation of its *racemic* analog. In comparison, complex $\mathbf{III_{Hf}}$ behaves vice versa where methylation of the *racemic* isomer is preferred by 11 kJ/mol over methylation of its *meso* counterpart. Since only complex $\mathbf{II_{Hf}}$ was experimentally able to undergo isomerization and considering this energetic discrepancy, we concluded the metal-chloride-TMA interaction to be a crucial step of the isomerization mechanism. According to the data presented, we propose a mechanism for the TMA-induced isomerization of methoxy-substituted *meso* metallocene complexes as depicted in Scheme 3—using *meso*-$\mathbf{I_{Hf}}$ as an example since the kinetic NMR data were gathered from this complex.

Our proposed reaction sequence starts with the coordination of TMA to *meso*-$\mathbf{I_{Hf}}$ to form $L_2ClHf(\mu\text{-}Cl)AlMe_3$ and the subsequent exchange of one methyl group to form $L_2ClHf(\mu\text{-}Me)AlMe_2Cl$. Although, as mentioned, DFT calculations revealed the chloride-substituted species to be energetically slightly favored over the methylated one, the data gathered from the kinetic ^{1}H NMR study clearly indicate that the reaction proceeds via the methyl-bridged species. The driving force of the reaction thus probably

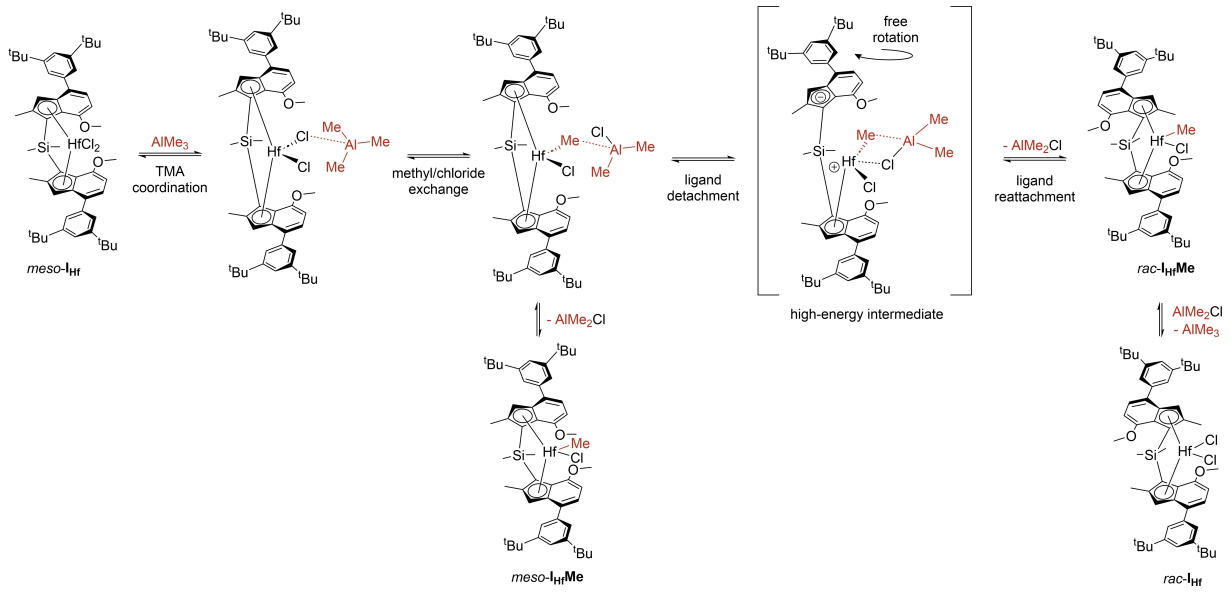

Scheme 3. Proposed TMA-induced isomerization mechanism of methoxy-substituted group IV metallocene complexes using *meso*-$\mathbf{I_{Hf}}$ as an example.

originates from this species being withdrawn from the $L_2ClHf(\mu\text{-}Cl)AlMe_3/L_2ClHf(\mu\text{-}Me)AlMe_2Cl$ equilibrium.

The complex/TMA adduct was stable enough to be detected in the corresponding LIFDI mass spectrum (Figure 5). This was an exciting observation considering the fact these types of interactions are usually regarded as dynamic and short-lived.[17] The detectability of this adduct via LIFDI-MS indicates the μ-Me coordination to be quite firm. We therefore hypothesized that the cleavage of the Hf–Cp bond necessary for an isomerization to take place might be enabled by the coordination of a second substituent from the Al atom to the Hf center to form a doubly bridged $LClHf(\mu\text{-}Cl)(\mu\text{-}Me)AlMe_2$ high-energy intermediate as depicted in Scheme 3. The arising donation of additional electron density to the central metal atom should partially compensate the formally cationic charge upon detachment of the Cp-ligand. From this intermediate, the ligand would be able to freely rotate and to be subsequently reattached to the central metal atom to form the thermodynamically favored *racemic* isomer. A similar mechanism has been proposed in the literature.[7a] DFT calculations proved the possibility of such a high-energy intermediate to exist for complex $\mathbf{II_{Hf}}$, its formation being endergonic by 160 kJ/mol. Optimization trials of an analog doubly-bridged $L_2ClHf(\mu\text{-}Cl)(\mu\text{-}Me)AlMe_2$ species with both Cp-ligands still attached to the central metal atom failed and yielded $L_2ClHf(\mu\text{-}Cl)AlMe_3$ in all cases, substantiating the need for one Cp-ligand to be detached. The geometry-optimized structure of this high-energy intermediate is shown in Figure 6.

Methylation of the *meso* isomers of complexes **III**–**V** (M: Zr, Hf) bearing no methoxy groups was also observed. However, the reaction stopped at the methylated complexes and no isomerization took place. In line with these observations is the elevated endergonicity of 196 kJ/mol for the analog high-energy intermediate of complex $\mathbf{III_{Hf}}$ to form from its parent compound. The higher energy difference of 36 kJ/mol compared to $\mathbf{II_{Hf}}$ highlights again the necessity and role of the methoxy groups in the aluminum-alkyl induced isomerization of the investigated group IV metallocene complexes.

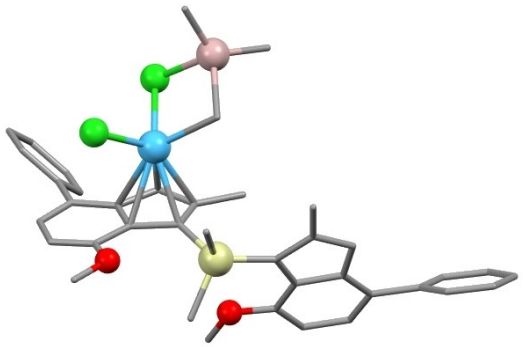

Figure 6. Geometry-optimized structure of the high-energy intermediate of $\mathbf{II_{Hf}}$ upon reaction with TMA and detachment of one ligand.

Conclusion

In summary, we improved and extended the scope of our previously introduced isomerization of hafnocene complex *meso*-$\mathbf{I_{Hf}}$ onto metallocene complexes with different ligand frameworks and zirconocene/MAO systems. We were therefore able to utilize *meso* metallocene complexes—that are generally considered waste—to produce isotactic polypropylene with macromolecular characteristics equal to iPP produced by the corresponding pure *racemic* isomers. This allowed for an increase of iPP per amount of ligand used for the metallocene syntheses by up to 400 %.

By progressively varying substituents on the indenyl moieties of the ligands, we were able to identify the methoxy substituents at position 7 to be the crucial factor for an isomerization to take place. DFT calculations revealed that the energies required to adapt the respective ligand conformations in the presence of these substituents differ by as much as 19 kJ/mol. Ligands bearing no methoxy groups exhibited no energetic differences in both conformers, and thus, it becomes evident that the driving force of the isomerization lies in these energetic discrepancies. Based on results gathered from ^{1}H and ^{29}Si NMR, as well as LIFDI-MS experiments, we proposed a mechanism of the TMA-induced isomerization. This mechanism involves an intermediate stabilized by a μ-Me and μ-Cl interaction of TMA with the central metal atom. From this intermediate, a rotation of one indenyl ligand to form the corresponding *racemic* isomer can take place. The proposed mechanism should yield the methylated compounds *meso*-$\mathbf{I_{Hf}Me}$ and *rac*-$\mathbf{I_{Hf}Me}$ as intermediary species and both were actually detected experimentally. Furthermore, two other feasible isomerization pathways were ruled out using DFT calculations, substantiating the proposed mechanism.

The facile and effective isomerization of 7-methoxy substituted group IV metallocene complexes—in combination with their outstanding polymerization performances—should steer the future design of this class of catalysts toward such in the scope of an energy- and atom-efficient polyolefin economy.

The authors have cited additional references within the Supporting Information.[18–32]

Acknowledgements

The authors would like to thank Patricia Aufricht, Cara Bommer, and Ruocheng Tang for help with the metallocene syntheses. Furthermore, they would like to thank Dr. Lucas Stieglitz and Magdalena Kleybolte for proofreading the manuscript, as well as Dr. Sergei Vagin, Dr. Sven Krüger, and Patrick Mollik for valuable discussions. The authors also gratefully acknowledge the computational and data resources provided by the Leibniz Supercomputer Center (www.lrz.de). Open Access funding enabled and organized by Projekt DEAL.

Conflict of Interest

The authors declare no conflict of interest.

Data Availability Statement

SC-XRD data is available from www.ccdc.cam.ac.uk/ products/csd with deposition numbers 2308439 (*rac*-$\mathbf{V_{Hf}}$) and 2308440 (*rac*-$\mathbf{II_{Zr}}$).[33]

Keywords: density functional calculations · isomerization · metallocenes · olefin polymerization · polypropylene

[1] a) G. Natta, *Angew. Chem.* **1956**, *68*, 393–403; b) K. Ziegler, E. Holzkamp, H. Breil, H. Martin, *Angew. Chem.* **1955**, *67*, 541–547.
[2] W. Kaminsky, K. Külper, H. H. Brintzinger, F. R. W. P. Wild, *Angew. Chem. Int. Ed. Engl.* **1985**, *24*, 507–508.
[3] a) P. S. Kulyabin, G. P. Goryunov, M. I. Sharikov, V. V. Izmer, A. Vittoria, P. H. M. Budzelaar, V. Busico, A. Z. Voskoboynikov, C. Ehm, R. Cipullo, D. V. Uborsky, *J. Am. Chem. Soc.* **2021**, *143*, 7641–7647; b) N. M. R. Machat, D. Lanzinger, A. Pöthig, B. Rieger, *Organometallics* **2017**, *36*, 399–408; c) A. Vittoria, G. Urciuoli, S. Costanzo, D. Tammaro, F. D. Cannavacciuolo, R. Pasquino, R. Cipullo, F. Auriemma, N. Grizzuti, P. L. Maffettone, V. Busico, *Macromolecules* **2022**, *55*, 5017–5026.
[4] A. Schöbel, E. Herdtweck, M. Parkinson, B. Rieger, *Chem. Eur. J.* **2012**, *18*, 4174–4178.
[5] P. S. Kulyabin, V. V. Izmer, G. P. Goryunov, M. I. Sharikov, D. S. Kononovich, D. V. Uborsky, J. A. M. Canich, A. Z. Voskoboynikov, *Dalton Trans.* **2021**, *50*, 6170–6180.
[6] J. A. Ewen, *J. Am. Chem. Soc.* **1984**, *106*, 6355–6364.
[7] a) R. M. Buck, N. Vinayavekhin, R. F. Jordan, *J. Am. Chem. Soc.* **2007**, *129*, 3468–3469; b) W. Kaminsky, A.-M. Schauwienold, F. Freidanck, *J. Mol. Catal. A* **1996**, *112*, 37–42.
[8] L. Stieglitz, T. M. Lenz, A. Saurwein, B. Rieger, *Angew. Chem. Int. Ed.* **2022**, *61*, e202210797.
[9] a) J. Karger-Kocsis, T. Bárány, *Switzerland: Springer Nature* **2019**; b) V. V. Izmer, A. Y. Lebedev, D. S. Kononovich, I. S. Borisov, P. S. Kulyabin, G. P. Goryunov, D. V. Uborsky, J. A. M. Canich, A. Z. Voskoboynikov, *Organometallics* **2019**, *38*, 4645–4657; c) A. Vittoria, G. P. Goryunov, V. V. Izmer, D. S. Kononovich, O. V. Samsonov, F. Zaccaria, G. Urciuoli, P. H. Budzelaar, V. Busico, A. Z. Voskoboynikov, *Polymer* **2021**, *13*, 2621.
[10] a) M. Nikulin, A. Tsarev, A. Lygin, A. Ryabov, I. Beletskaya, A. Voskoboinikov, *Russ. Chem. Bull.* **2008**, *57*, 2298–2306; b) W. Spaleck, M. Antberg, J. Rohrmann, A. Winter, B. Bachmann, P. Kiprof, J. Behm, W. A. Herrmann, *Angew. Chem.* **1992**, *104*, 1373–1376.
[11] M. Muhr, P. Heiß, M. Schütz, R. Bühler, C. Gemel, M. H. Linden, H. B. Linden, R. A. Fischer, *Dalton Trans.* **2021**, *50*, 9031–9036.
[12] K. P. Bryliakov, E. P. Talsi, A. Z. Voskoboynikov, S. J. Lancaster, M. Bochmann, *Organometallics* **2008**, *27*, 6333–6342.
[13] V. Busico, R. Cipullo, R. Pellecchia, G. Talarico, A. Razavi, *Macromolecules* **2009**, 1789–1791.
[14] W. Kaminsky, H. Sinn, *Polyolefins: 50 years after Ziegler and Natta II: Polyolefins by Metallocenes and Other Single-Site Catalysts* **2013**, 1–28.
[15] R. Tanaka, T. Kawahara, Y. Shinto, Y. Nakayama, T. Shiono, *Macromolecules* **2017**, *50*, 5989–5993.
[16] a) R. D. Shannon, *Acta Crystallogr. Sect. A* **1976**, *32*, 751–767; b) R. T. Shannon, C. T. Prewitt, *Acta Crystallogr. Sect. B* **1969**, *25*, 925–946.
[17] a) S. Beck, H. H. Brintzinger, *Inorg. Chim. Acta* **1998**, *270*, 376–381; b) U. Wieser, D. Babushkin, H.-H. Brintzinger, *Organometallics* **2002**, *21*, 920–923.
[18] H. H. Brintzinger, D. Fischer, R. Mülhaupt, B. Rieger, R. M. Waymouth, *Angew. Chem. Int. Ed.* **1995**, *34*, 1143–1170.
[19] B. Coto, J. M. Escola, I. Suárez, M. J. Caballero, *Polym. Test.* **2007**, *26*, 568–575.
[20] W. A. Herrmann, J. Rohrmann, E. Herdtweck, W. Spaleck, A. Winter, *Angew. Chem. Int. Ed.* **1989**, *28*, 1511–1512.

[21] W. Spaleck, F. Kueber, A. Winter, J. Rohrmann, B. Bachmann, M. Antberg, V. Dolle, E. F. Paulus, *Organometallics* **1994**, *13*, 954–963.
[22] a) D. Andrae, U. Haeussermann, M. Dolg, H. Stoll, H. Preuss, *Theor. Chim. Acta* **1990**, *77*, 123–141; b) F. Furche, R. Ahlrichs, C. Hättig, W. Klopper, M. Sierka, F. Weigend, *Wiley Interdiscip. Rev.: Comput. Mol. Sci.* **2014**, *4*, 91–100.
[23] J. Tomasi, M. Persico, *Chem. Rev.* **1994**, *94*, 2027–2094.
[24] J. Ho, A. Klamt, M. L. Coote, *J. Phys. Chem. A* **2010**, *114*, 13442–13444.
[25] S. Miertuš, E. Scrocco, J. Tomasi, *Chem. Phys.* **1981**, *55*, 117–129.
[26] G. M. Sheldrick, *Acta Crystallogr. Sect. A* **2015**, *71*, 3–8.
[27] G. M. Sheldrick, *Acta Crystallogr. Sect. C* **2015**, *71*, 3–8.
[28] C. B. Hübschle, G. M. Sheldrick, B. Dittrich, *J. Appl. Crystallogr.* **2011**, *44*, 1281–1284.
[29] *International Tables for Crystallography, Vol. C* (Ed.: A. J. Wilson), Kluwer Academic Publishers, Dordrecht, The Netherlands **1992**, Tables 6.1.1.4 (pp. 500–502), 4.2.6.8 (pp. 219–222), and 4.2.4.2 (pp. 193–199).
[30] C. F. Macrae, I. J. Bruno, J. A. Chisholm, P. R. Edgington, P. McCabe, E. Pidcock, L. Rodriguez-Monge, R. Taylor, J. van de Streek, P. A. Wood, *J. Appl. Crystallogr.* **2008**, *41*, 466–470.
[31] D. Kratzert, I. Krossing, *J. Appl. Crystallogr.* **2018**, *51*, 928.
[32] A. L. Spek, *Acta Crystallogr. Sect. D* **2009**, *65*, 148–155.
[33] a) P. C. Möhring, N. J. Coville, *Coord. Chem. Rev.* **2006**, *250*, 18–35; b) R. M. Shaltout, J. Y. Corey, N. P. Rath, *J. Organomet. Chem.* **1995**, *503*, 205–212; c) Deposition Numbers 2308439 (for *rac*-$\mathbf{V_{Hf}}$) and 2308440 (for *rac*-$\mathbf{II_{Zr}}$) contain the supplementary crystallographic data for this paper. These data are provided free of charge by the joint Cambridge Crystallographic Data Centre and Fachinformationszentrum Karlsruhe Access Structures service.

Manuscript received: April 10, 2024
Accepted manuscript online: July 7, 2024
Version of record online: August 20, 2024